Received: 24 July 2019 | Revised: 30 October 2019 | Accepted: 13 November 2019

DOI: 10.1096/fj.201901858RR

RESEARCH ARTICLE

THE FASEB JOURNAL

A human co-culture cell model incorporating microglia supports glioblastoma growth and migration, and confers resistance to cytotoxics

Diana M. Leite[1] | **Barbara Zvar Baskovic**[2] | **Prospero Civita**[1,3] | **Catia Neto**[4] | **Mark Gumbleton**[4] | **Geoffrey J. Pilkington**[1]

[1]Brain Tumour Research Centre, Institute of Biological and Biomolecular Sciences (IBBS), School of Pharmacy and Biomedical Sciences, University of Portsmouth, Portsmouth, UK

[2]Biotehniska Fakulteta, Univerza v Ljubljana, Ljubljana, Slovenia

[3]Genomics Section, Fondazione Pisana per la Scienza ONLUS, Pisa, Italy

[4]School of Pharmacy and Pharmaceutical Sciences, University of Cardiff, Cardiff, UK

Correspondence
Geoffrey J. Pilkington, Brain Tumour Research Centre, Institute of Biological and Biomedical Sciences (IBBS), School of Pharmacy and Biomedical Sciences, University of Portsmouth, White Swan Road, Portsmouth PO1 2DT, UK.
Email: geoff.pilkington@port.ac.uk

Present address
Diana M. Leite, Department of Chemistry, University College London, London, UK

Funding information
Jake McCarthy Foundation, Grant/Award Number: N/A; Brain Tumour Research, Grant/Award Number: N/A

Abstract

Despite the importance of the tumor microenvironment in regulating tumor progression, few in vitro models have been developed to understand the effects of non-neoplastic cells and extracellular matrix (ECM) on drug resistance in glioblastoma (GBM) cells. Using CellTrace-labeled human GBM and microglial (MG) cells, we established a 2D co-culture including various ratios of the two cell types. Viability, proliferation, migration, and drug response assays were carried out to assess the role of MG. A 3D model was then established using a hyaluronic acid-gelatin hydrogel to culture a mixture of GBM and MG and evaluate drug resistance. A contact co-culture of fluorescently labeled GBM and MG demonstrated that MG cells modestly promoted tumor cell proliferation (17%-30% increase) and greater migration of GBM cells (>1.5-fold increase). Notably, the presence of MG elicited drug resistance even when in a low ratio (10%-20%) relative to co-cultured tumor cells. The protective effect of MG on GBM was greater in the 3D model (>100% survival of GBM when challenged with cytotoxics). This new 3D human model demonstrated the influence of non-neoplastic cells and matrix on chemoresistance of GBM cells to three agents with different mechanisms of action suggesting that such sophisticated in vitro approaches may facilitate improved preclinical testing.

KEYWORDS

3D co-culture, drug resistance, human serum, hyaluronic acid hydrogel

Abbreviations: 3D, 3-dimensional; BBB, blood-brain barrier; BSA, bovine serum albumin; CCL22, C-C motif chemokine ligand 22; CFSE, carboxyfluorescein succinimidyl ester; CLM, clomipramine; CXCL10, C-X-C motif chemokine ligand 10; DMEM, Dulbecco's modified eagle medium; ECM, extracellular matrix; eGFP, enhanced green fluorescent protein; GAGs, glycosaminoglycans; GAPDH, glyceraldehyde 3-phosphate dehydrogenase; GBM, glioblastoma multiforme; HBSS, Hank's balanced salt solution; IL, interleukin; IFN-γ, interferon gamma; iPSCs, induced pluripotent stem cells; LPS, lipopolysaccharide; MG, microglia; NCBI, national centre for biotechnology information; PCR, polymerase chain reaction; RT-qPCR, quantitative real-time polymerase chain reaction; SR-A, scavenger receptor-A; STAT, signal transducer and transcription; STR, short tandem repeat (STR); TGF-β, transforming growth factor beta; TLR4, toll-like receptor 4; TMZ, temozolomide; TNF-α, tumor necrosis factor alpha; TGM2, transglutaminase 2 (TGM2); VCR, vincristine.

1 | INTRODUCTION

Glioblastoma multiforme (GBM), grade IV glioma, is the most common and malignant form of primary brain cancer accounting for nearly 45% of all gliomas.[1] Although the addition of radiotherapy and chemotherapy to a resection surgery modestly improves the survival, GBM is inherently resistant to treatments resulting in a median survival of 14.6 months.[2]

GBM cells dynamically respond to their local microenvironment, thereby affecting tumor cell behavior.[3,4] Important components of the tumor microenvironment include: (a) non-neoplastic cells near or within the tumor, (b) extracellular matrix, which is a scaffold surrounding the tumor cells enriched in hyaluronic acid, and (c) soluble signals such as growth and differentiation factors.[5,6] Non-neoplastic cells associated with GBM are glial, immune, microglial, vascular endothelial, pericytic and neuronal in nature. Glial cells—predominantly astrocytes—are the most abundant cells in the brain.[7]

Microglia (MG) cells are important for maintaining brain homeostasis. In the resting state, they act as a sentinel, and with activation show plasticity along with two broadly defined phenotypes as: (a) pro-inflammatory, classical, and anti-tumoral or (b) anti-inflammatory, alternative, or pro-tumoral. These two subpopulations differ with respect to cytokine and chemokine production, receptor expression, and effector function.[8-11] MG, which can comprise up to 35%-50% of the tumor,[8] have been shown in a few reports to stimulate proliferation and invasion of GBM cells in vitro and in vivo.[12-15] However, little is known whether MG cells mediate effects on the response of GBM to cytotoxics.

In addition to these non-neoplastic cells, a 3D extracellular matrix has been reported to influence tumor cell behavior and response to cytotoxics, when compared to the standard 2D monoculture.[16-18] Comprising ~20% of the tissue volume, brain extracellular matrix contains few fibrous proteins and high amounts of proteoglycans, glycosaminoglycans (GAGs), and glycoproteins.[3,4] Hyaluronic acid—a negatively charged, unbranched GAG—is highly abundant in the brain matrix. In the healthy brain, high molecular weight (10^6 Da) hyaluronic acid chains act as the organizational center of the matrix, interacting with proteins to create a hydrogel-like mesh.[19]

In GBM, hyaluronic acid matrix is upregulated and contributes to many phenotypic alterations associated with tumor progression, including cell proliferation, invasion, and drug resistance.[20,21] The soluble signals and differentiation factors in the serum-supplemented media also influence cell growth and interaction with exogenous factors.[22] In fact, it has been revealed that human serum stimulates the growth of human mammary tumor cells in culture,[22] thus implying the significance of human serum in modeling a tumor microenvironment. In our laboratories, human serum supplementation has also been shown to modulate both protein and gene expression in human biopsy-derived GBM cells as well as to influence cell shape and proliferation.[23]

Although various microenvironmental features strongly influence GBM, current models for therapeutic testing fail to account for the complex microenvironment surrounding the tumor, and hence may not adequately reflect clinical outcomes. Multiple studies are focused on GBM-extracellular matrix or GBM-non-neoplastic cell (such as astrocytes) interactions using 2D in vitro platforms, however few models have been established to study the role of the non-neoplastic cells, particularly MG, on GBM in a 3D extracellular matrix context. Since within our laboratories we have considerable experience of 3D human cell in vitro modeling in the context of GBM invasion,[24] blood-brain barrier mediated drug delivery,[25] and cancer metastasis,[26,27] we decided to begin a multistage program of developing such 3D models for preclinical drug testing of GBM using all human, multicellular, in vitro conditions. In the initial study, which we report here, we explored the influence of MG on proliferation, migration, and response to temozolomide (TMZ), clomipramine (CLM), and vincristine (VCR) on three human GBM cell lines in human serum-supplemented conditions. The three agents used in our studies have been previously used widely in various 2D in vitro studies using both rat or mouse and human cells in the context of GBM therapies. Moreover, human mouse models have been used to assess tricyclic agents,[28-30] TMZ[31] and VCR.[32] Co-cultures of human MG and GBM were carried out in 2D to comprehend the effect of MG in GBM, and then to mimic the characteristic environment of GBM, this co-culture of GBM and MG was explored in a 3D hyaluronic acid-based hydrogel. Therefore, a 2D co-culture allowed us to elucidate how the presence of MG cells modulates the response to clinically relevant drugs in a panel of GBM tumor cells, while a 3D co-culture mimics the tumor microenvironment appearing as a powerful platform for drug screening.

2 | METHODS

2.1 | Ethics statement

A biopsy from a glioma patient was resected at King's College Hospital, London, under Ethics permission LREC00-173/11/SC/0048 in accordance with a National Research Ethics Service and the study was approved through ethic committees for the University of Portsmouth and King's College Hospital. Patient signed an informed written consent prior to surgery.

2.2 | Cell culture

Three human GBM cell lines were used in this study (U-87 MG, SNB-19 and UP-007) (Table 1). U-87 MG cells were

TABLE 1 Details of the GBM cell lines

Cell line	Sex	Age	Passage[a]	Location	Other
U-87MG	Male	–	28-31	–	–
SNB-19	Male	47	53-56	Left parietal-occipital lobe	–
UP-007	Male	71	46-50	–	Wild-type IDH1

[a]Cell passage of U-87MG and SNB-19 refers to the numbers given by the suppliers and, since these cells have been grown for several decades p-numbers would, realistically be far higher than the passage reported on the table. UP-007, as an in-house biopsy-derived cell line, is only cell population which carries a real authenticated passage number and is thus more heterogeneous in nature.

obtained from the European Collection of Cell Culture, SNB-19 were obtained from DSMZ German Brain Tumour Bank, and UP-007 cells were established in house from a GBM biopsy resected at King's College Hospital. A human MG cell line, CHME3, an SV40 large T antigen immortalized human foetal microglia cell line,[33] was kindly provided by Prof Brian Bigger from University of Manchester. Both GBM and MG cells were cultured in Dulbecco's modified Eagle medium (DMEM, Gibco, Fisher Scientific, Loughborough, UK) supplemented with 10% (v/v) of human serum (Sigma-Aldrich, Dorset, UK). All cells were maintained at 37°C in a humidified incubator with 5% CO_2. Media was changed every 2-3 days, and subculturing was carried out by washing cells with Hank's balanced salt solution (HBSS, Gibco, Fisher Scientific, Loughborough, UK) and incubation with TrypLE express enzyme (Gibco, Fisher Scientific, Loughborough, UK).

All cell lines were routinely and regularly screened for the presence of mycoplasma using the commercially available MycoAlert assay kit (Lonza, Basel, Switzerland), as described by the manufacturers' instructions. For DNA isolation and cell line authenticity, genomic DNA was isolated from cell pellets (5×10^6 cells) using QiaAMP DNA Mini kit, (Qiagen, Manchester, UK) as described by the manufacturers' instructions. DNA authentication was carried out using Geneprint 10 system (Promega, Southampton, UK) according to manufacturers' instructions. DNA (15 ng) was subject to polymerase chain reaction (PCR) amplification in the presence of short tandem repeat (STR) loci, consisting of the following primer pairs: TH01, D21S11, D5S818, D13S317, D7S820, D16S539, CSF1PO, vWA, TPOX, and Amelogenin, for gender identification. Amplification was carried out as follows: 96°C for 1 minute, followed by 30 cycles of 94°C for 10 seconds, 59°C for 1 minute, and 72°C for 30 seconds, followed by 60°C for 10 minutes, 4°C soak. Fragment length analysis was done using fluorescence detection following microcapillary electrophoresis (Eurofins Genomics, Ebersberg, Germany), and DNA profile was compared with known database standards. We also DNA fingerprinted cells using an *in house*-developed microfluidic electrophoresis system incorporating a 2100 Bioanalyzer (Agilent Technologies, Santa Clara, CA, USA) to analyze short tandem repeat PCR fragments from 10 human genomic loci of human cell lines.[34]

2.3 | Cell labeling

Cell labeling optimization screening was performed with all GBM cells and MG using the CellTrace carboxyfluorescein succinimidyl ester (CFSE) and a CellTrace Far Red (Invitrogen, Fisher Scientific, Loughborough, UK), respectively. For the labeling, cells were incubated with TrypLE Express for 3 minutes, centrifuged, and resuspended in 1 mL of HBSS (with Ca^{2+} and Mg^{2+}). GBM cells were incubated with CellTrace CFSE (5-10 μM) and CHME3 cells incubated with CellTrace Far Red (1 μM) in HBSS for 20 minutes at 37°C. Afterward, to remove unconjugated CellTrace, cell suspensions were incubated with DMEM supplemented with 5% (v/v) human serum for 5 minutes at room temperature. Subsequently, both cells were centrifuged, resuspended in complete DMEM, and analyzed in a Counter II FL Automated Cell Counter to assess the number of cells and viability.

2.3.1 | Cell labeling efficacy

To evaluate the efficacy of the labeling, $CFSE^+$ GBM cells and Far Red^+ CHME3 cells were seeded at 20 000 cells/cm^2 in a 24-well plate in DMEM supplemented with 10% (v/v) human serum and allowed to grow up to 9 days. On Days 1, 3, 5, 7, and 9, cells were analyzed by flow cytometry to quantify the remaining percentage of labeled cells. $CFSE^+$ GBM cells (U-87 MG, SNB-19, and UP-007) were detected using the blue 488 laser and the 530/30 channel (FL1). Far Red^+ MG cells were excited with the red laser 635 and detected with a 661/16 channel (FL4). Non-stained cells were included as a control. Cells were analyzed in the FACS Calibur flow cytometer (BD Biosciences, Wokingham, UK) collecting at least 10,000 events. The FlowJo software was used for analysis of the data.

2.3.2 | Cell viability

The effect of the CellTrace on the metabolic activity of GBM cells (CFSE) and MG (Far Red) was evaluated by the CellTiter 96 Cell Proliferation Assay (MTS, Promega, Southampton,

UK). CFSE$^+$ GBM (U-87MG, SNB-19, or UP-007) or Far Red$^+$ CHME3 cells were seeded at 20 000 cells/cm^2 in a 96-well plate in DMEM supplemented with 10% (v/v) human serum and allowed to grow up to 9 days. On specific time points, the MTS solution was added (20 µL) to each well, and cells were incubated at 37°C for 2 hours. Absorbance was measured at λ 492 nm using a POLARstar Omega microplate reader (BMG Labtech, Ortenberg, Germany). Non-stained cells were used as a control in each experiment.

2.4 | MG plasticity

MG were seeded at 20 000 cells/cm^2 and allowed to adhere for 24 hours. Afterward, the medium was replenished, and cells were treated for additional 48 hours with either 1 µg mL^{-1} of lipopolysaccharides (LPS) (Sigma, Gillingham, UK) plus 20 ng mL^{-1} of Interferon-ɣ (IFN-ɣ) (PeproTech Inc, New Jersey, USA) to drive the MG toward a pro-inflammatory phenotype or with 20 ng mL^{-1} of interleukin-4 (IL-4) (PeproTech Inc, New Jersey, USA) plus 20 ng mL^{-1} of interleukin-13 (IL-13) (PeproTech Inc, New Jersey, USA) to drive the MG toward an anti-inflammatory phenotype. Cells in standard culture conditions were used as a control.

2.4.1 | Quantitative real-time polymerase chain reaction

Total mRNA was isolated from CHME3 cells with RNeasy Mini Kit (Qiagen, Manchester, UK). Quantification and integrity of the extracted mRNA was performed by spectrophotometry with measurement of absorbance at 260 and 280 nm in a NanoVue Plus Spectrophotometer (GE Healthcare, Freiburg, Germany). The cDNA was synthesized from 1 µg of RNA by reverse transcription using the High-Capacity cDNA Reverse Transcription Kit (ABI Applied Biosystems, Life Technologies Europe, Bleiswijk, Netherlands) in a reaction volume of 20 µL. All primers designed for reference and target genes were based on sequences published on the GeneBank, National Centre for Biotechnology Information (NCBI). BLAST searches were performed to confirm the total gene specificity of the primer sequences. Primer sequences are listed in the Supplemental Table 1, and were obtained from Invitrogen (Life Technologies Limited, Paisley, UK). The RT-qPCR was performed in duplicate using PowerUP SYBR Green Master Mix (Applied Biosystems, Thermo Fisher Scientific Baltics UAB, Vilnius, Lithuania), a LightCycler 96 system (Roche, Mannheim, Germany), in a final volume of 12 µL containing 20 ng of cDNA, according to the following protocol: initial incubation at 50°C for 2 minutes plus 95°C for 2 minutes, followed by 45 cycles of 15 seconds at 95°C, 15 seconds at 60°C, and 60 seconds at 72°C, followed by melting curve with an increasing from 55 to 95°C. Normalization was performed using the reference gene glyceraldehyde-3-phosphate dehydrogenase (GAPDH) and the ΔΔCt method.[35]

2.4.2 | Western blot

After 48 hours of polarization, the MG cells were lysed using ice-cold RIPA lysis and extraction buffer (Life Technologies Europe BV, Bleiswijk, Netherlands) with 1% (v/v) of Halt Protease Inhibitor Cocktail (Thermo Fisher Scientific, Pierce Biotechnology, Rochford, USA) for 30 minutes on ice, then centrifuged at 13 000 *g* for 10 minutes at 4°C. Total protein concentration was determined using Coomassie Plus Reagent (Life Technologies Europe BV, Bleiswijk, Netherlands). The total protein (20 µg) was denatured using NuPAGE sample reducing agent and NuPAG LDS sample buffer (Life Technologies Europe BV, Bleiswijk, Netherlands) for 5 minutes at 95ºC, resolved on a Mini-PROTEAN TGX 12% (w/v) SDS polyacrylamide Precast Gel (Bio-Rad, Hertfordshire, UK), and immunoblotted onto a 0.2-µm nitrocellulose membrane (Schleicher and Schuell, Dassel, Germany). The membranes were blocked for 1 hour with blocking buffer consisting of 5% (w/v) bovine serum albumin (BSA, phosphorylated forms) or 5% (w/v) fat-free dry milk (total forms) in Tris-buffered saline (TBS)-Tween 20 (0.05% (w/v)) (TBS-T, pH 7.5) and then incubated with the primary antibody of choice for 16 hours at 4°C (1:1000 in 5% (w/v) BSA). All primary antibodies were obtained from Cell Signaling (New England Biolabs, Hertfordshire, UK): phospho-STAT1 (Tyr701) (58D6), STAT1 (D1K9Y), phospho-NF-κB p65 (Ser536) (93H1), NF-κB p65 (E498), phospho-STAT6 (Tyr641), STAT6, phospho-STAT3 (Tyr705) (D3A7), STAT3, and GAPDH (14C10). Following primary antibody incubation, membranes were washed (3 times for 5 minutes) in TSB-T and incubated for 1 hour at room temperature with the required secondary anti-rabbit IgG, HRP-linked antibody (Cell Signaling, New England Biolabs, Hertfordshire) diluted 1:10 000 in blocking buffer. Membranes were again washed (6 times for 5 minutes) in TSB-T and signals detected using either in a SuperSignal WEST DURA or in a FEMTO chemiluminescent substrate (Pierce, Chester, UK). Signals were captured on ChemiDocTM XRS+ (BIORAD, Hertfordshire, UK).

2.4.3 | Cytokine array

Soluble factors secreted by MG were evaluated by Human XL Cytokine Array (R&D Systems, Minneapolis, USA). Cell culture supernatants were collected after 48 hours of

polarization, and the unstimulated cells were used as a control. The collected cell culture supernatants were centrifuged to remove any particles and use for analysis immediately according to the kit instructions.

2.5 | 2D co-cultures: Cell viability and proliferation

Co-cultures of the GBM (U-87 MG, SNB-19 or UP-007) and MG were established by seeding both cell lines in a 24-well plate at a final density of 20 000 cells/cm^2. CFSE$^+$ GBM and Far Red$^+$ CHME3 cells were cultured either alone (40 000 cells) or cultured in co-culture at the following ratio of GBM to CHME3 cells: 90:10 (36 000:4000), 80:20 (32 000:8000), or 50:50 (40 000:40 000). Cells were allowed to grow in close contact for 3 days.

2.5.1 | Cell imaging

Co-cultures were cultured for 3 days and, subsequently, fixed using paraformaldehyde solution, 4% (w/v), for 15 minutes at room temperature. Cells were washed and stored at 4°C. Imaging was carried in a LSM719 confocal laser-scanning microscope (Zeiss, Oberkochen, Germany) using a Plan Apochromatic 20×/0.8 M27 objective (NA 0.8). All images were acquired using sequential acquisition of the different channels to avoid cross-talk between CellTrace with a pinhole adjusted to one airy unit. Images were processed with Zen 2009 Light Edition (Zeiss, Oberkochen, Germany).

2.5.2 | Cell viability

To evaluate viability of the cells in co-culture (GBM and CHME3), cells were incubated with TrypLE express enzyme for ~3 minutes, centrifuged, and resuspended in HBSS. Propidium iodide (Sigma-Aldrich, Dorset, UK) was added at the final concentration of 50 μg mL^{-1} and incubated for 5 minutes protected from the light. Cells were washed with HBSS and analyzed in FACS Calibur flow cytometer, as previously described. In addition to the aforementioned channels, propidium iodide-positive cells were detected using the blue 488 laser and the 630/30 channel (FL3). FlowJo software was used for analysis of the data.

2.5.3 | Cell proliferation

Cell proliferation was quantified by relation to the inverse of the fluorescence intensity of CFSE$^+$ GBMs and Far Red$^+$ CHME3. Both CellTrace molecules readily diffuse into cells and bind covalently to intracellular amines in proteins resulting in stable, well-retained fluorescent staining. The fluorescence intensity of the CellTrace is diminished with an increase of cell division as the reagent is passed through generations resulting in an inverse correlation between fluorescence intensity and cell proliferation. Thus, cells were analyzed by flow cytometry, as previously described, and using FlowJo software fluorescence intensity for each channel (FL1 or FL4) was obtained. Proliferation was calculated in relation to a control of cells growing in monoculture according to Equation (1):

$$\text{Proliferation (\%)} = \left(\frac{1}{(A/B)}\right) \times 100 \quad (1)$$

where A represents the cells growing in a co-culture (90:10, 80:20, 50:50 ratio of GBM to MG) and B is the control of cells growing in the monoculture (GBM or MG). The cell proliferation is expressed in function of the cells growing in a monoculture.

2.6 | 2D co-cultures: Cell migration

Linear cell migration was evaluated using a scratch-wound assay. Cells, either in a mono- or co-culture, were seeded at 100 000 cells/cm^2 in a 24-well plate and allowed to grow to a confluent monolayer over 24 hours. Afterward, a linear scratch was done using a 200 μL pipette tip. Following injury, wound closure was observed using EVOS FL Auto 2 Cell Imaging System (Fisher Scientific, Loughborough, UK) equipped with a cell imaging chamber under a humidified atmosphere (37°C, 5% CO_2). Images were acquired every 30 minutes over a period of 24 hours. Image analysis was performed using *Image J*, and rate of closure (μm/hour) was calculated by plotting distance of the wound gap *versus* time at different time points (0, 4, 8, 12, and 18 hours).

Cell migration was evaluated using a Transwell assay (8 μm pore size, a polycarbonate membrane, Corning, Loughborough, UK). Briefly, GBM cells (U-87 MG, SNB-19 or UP-007) were seeded in the upper compartment of a Transwell at 100 000 cells/cm^2 and maintained in a monoculture or in co-culture with CHME3 cells seeded in a 24-well plate at 100 000 cells/cm^2. After a co-culture for 24 hours, cells on the top compartment were removed and the Transwells were fixed in 70% (v/v) ethanol for 10 minutes. Transwells were allowed to dry for 10 minutes and stained with a 0.2% (w/v) Crystal Violet (ACROS Organics, Loughborough, UK) solution for 10 minutes at room temperature. The migrating GBM cells accumulating on the other side of the Transwell membrane were quantified using ImageJ. Threshold was

attuned and particle analysis was performed to obtain the total number of cells.

2.7 | 2D co-cultures: Drug response

GBM (U-87 MG, SNB-19 or UP-007) or CHME3 cells were seeded at 20 000 cells/cm^2 in a 96-welll plate and allowed to grow for 24 hours. Subsequently, the cells were treated with the cytotoxics: temozolomide (TMZ, Sigma-Aldrich, Dorset, UK), clomipramine (CLM, Sigma-Aldrich, Dorset, UK), or vincristine (VCR, Tocris, Bristol, UK) to calculate an IC_{50} value for each cell line. TMZ was dissolved in dimethyl sulfoxide at 1 mM, and working solutions were prepared from 200 to 1000 μM in DMEM. CLM was dissolved at 50 mM in water, and solutions were prepared at concentrations ranging 20-100 μM in DMEM. VCR sulfate was dissolved in water at 1 mM and working solutions were used from 2 to 10 μM in DMEM. After drug treatment, cells were incubated for 2 days, and viability was measured by CellTiter 96 Cell Proliferation Assay, as previously described. IC_{50} values were calculated using GraphPad Prism 7.03 software (GraphPad, California, USA).

To evaluate the influence of MG in GBM drug response, co-cultures in 2D were established as previously described, and cells were treated with TMZ (400 μM), CLM (20 μM) or VCR (2 μM). Following 48 hours of drug treatment, cells were analyzed by flow cytometry using a FACS Calibur collecting 10 000 events. The FlowJo software was used for analysis of the data, and cell proliferation was calculated using Equation (1). Untreated cells were used as a negative control and unlabeled cells were used as a control for the flow cytometry analysis.

2.8 | 3D co-cultures: Cell viability and proliferation

Cells were grown, either in mono- or co-culture, in a 3D HyStem-HP hyaluronic acid-based hydrogel (Sigma-Aldrich, Dorset, UK). HyStem-HP hydrogel is formed when the crosslinking agent Extralink (polyethylene glycol diacrylate M_w 3400 g/mol) is added to a mixture of HyStem-HP (thiol-modified hyaluronan) and Gelin-S (thiol-modified gelatin). Hydrogel was prepared according to the manufacturers' instructions. Both GBM (UP-007) and MG cells were grown in monoculture or in a co-culture at the ratio of 50:50 in the hyaluronic acid-based hydrogel. Briefly, UP-007 and CHME3 cells were labeled with CellTrace CFSE and Far Red, respectively, and encapsulated within the liquid hydrogel precursor solution at 1×10^6 cells mL^{-1}.[36] Hydrogels were allowed to polymerise for 20 minutes, and then complete DMEM media was added to each well. Cells in 3D were allowed to grow for 3 days.

2.8.1 | Cell viability

To evaluate the cell viability within the hydrogel, HyStem-HP was prepared and cells were mixed with the liquid precursor solution (50 μL hydrogel per well in 96-welll plate, 50 μL of DMEM). Cells were allowed to grow for 3 days, and CellTiter 96 Assay was carried out as described previously. Cell viability was additionally quantified by staining with propidium iodide (Sigma-Aldrich, Dorset, UK). The HyStem-HP hydrogel containing cells (UP-007, CHME-3 or UP-007:CHME3 at 50:50) was dispensed in μ-slide 18-well flat (IBIDI, Glasgow, UK) (15-μL hydrogel per well, 15 μL of DMEM), and cells allowed to grow for 3 days. Cells were incubated with propidium iodide solution (50 μg mL^{-1}) for 10 minutes at 37°C for detection of dead cells. After incubation, the cells were washed with phosphate-buffered saline (PBS) and observed under the LSM710 confocal laser microscope.

2.8.2 | Cell proliferation

The HyStem-HP hydrogel containing cells (UP-007, CHME-3 or UP-007:CHME3 at 50:50) was dispensed in μ-slide 18-well flat slide (IBIDI, Glasgow, UK) (15-μL hydrogel per well in 15 μL of DMEM), and cells allowed to grow for 3 days. Afterward, the cells were imaged under a LSM710 confocal laser microscope. Images were obtained from three replicates. Cell fluorescence intensity was quantified using ImageJ by obtaining integrated density of CFSE$^+$ cells.[37]

2.9 | 3D co-cultures: Drug response

To evaluate the influence of MG in GBM drug response when in 3D, co-cultures were established either in a 96-well plate (50 μL hydrogel per well, 50 μL of DMEM) or in 18 well-flat slide (15-μL hydrogel per well in 15 μL of DMEM) containing 1×10^6 cells mL^{-1} of gel. GBM cells were either cultured in monoculture or co-culture at a ratio of 50:50 with MG. Hydrogels were prepared and dispensed in the wells, and cells were allowed to grow for 24 hours within the hydrogel. Afterward, TMZ (400 μM), CLM (20 μM) or VCR (2 μM) was added to each well and cells incubated for 48 hours. Untreated cells were used as a control for each model (2D or 3D in a mono- or co-culture). Following the 48 hours, CellTiter 96 assay was performed as previously described to determine the cell viability in each model. To

assess cell proliferation, cells cultured in an 18-well flat slide were observed under LSM710 confocal laser microscope, and fluorescence of $CFSE^+$ GBM cells was analyzed as aforementioned using ImageJ.

2.10 | Statistical analysis

The results are expressed as mean ± standard error of the mean (SEM). Comparisons between groups were obtained by One-Way ANOVA using Dunnett's post hoc test in the comparison to a control or Tukey's for multiple comparisons between groups in GraphPad Prism 7.03. A significance level of $P < .05$ was considered statistically significant. In each experiment, N = 3 replicates for each condition and displayed data represent the mean of three independent experiments.

3 | RESULTS

3.1 | Optimization of the labeling of GBM and MG cells

In order to establish co-cultures to further elucidate the influence of MG on the behavior of GBM, the labeling of each cell type was optimized using CellTrace dyes. Three GBM cell lines (U-87 MG, SNB-19, UP-007) were stained using CFSE CellTrace and, as depicted on the Figure 1A,B, the

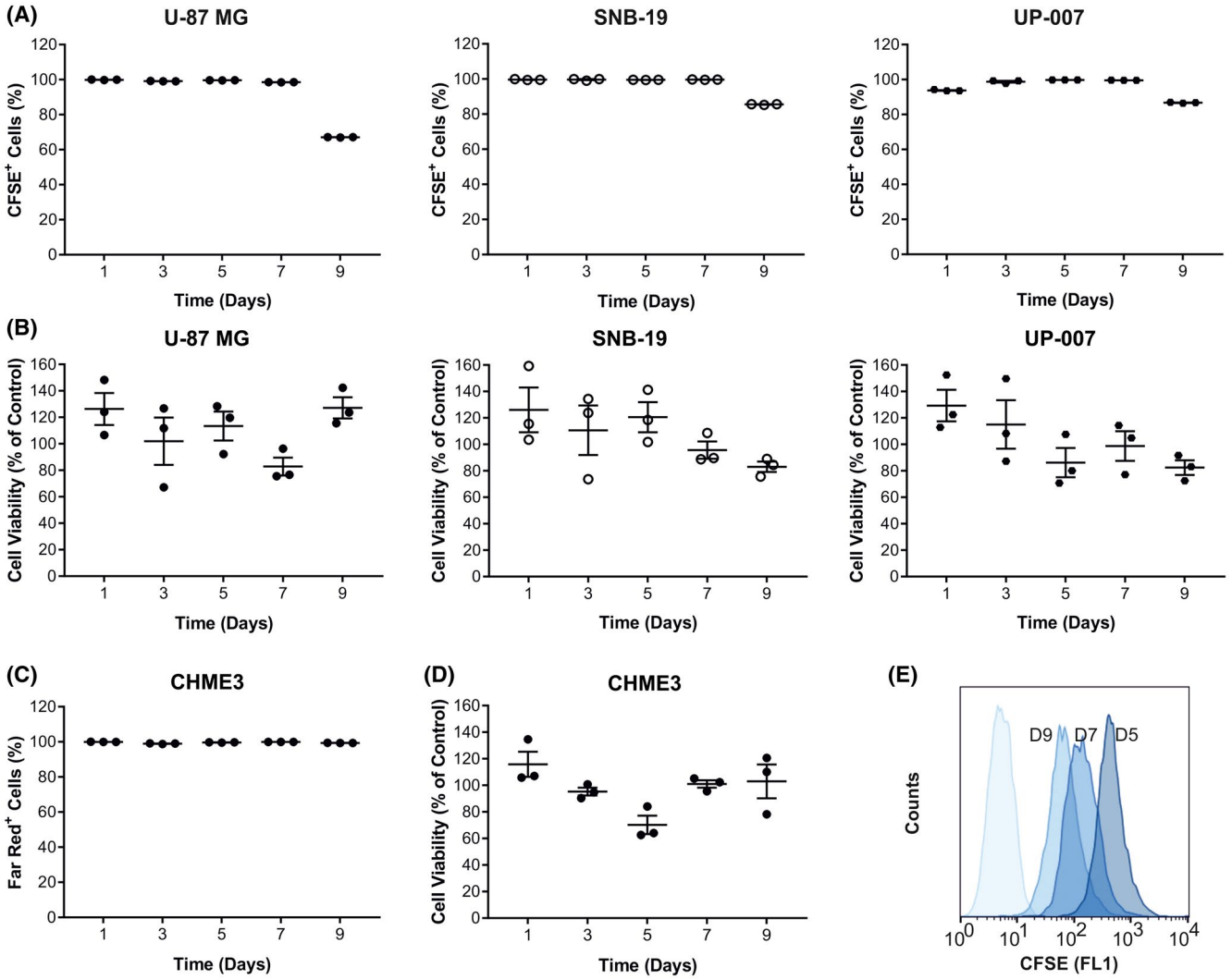

FIGURE 1 Labeling and viability of GBM and MG cells marked with CellTrace. A, Percentage of $CFSE^+$ U-87 MG, SNB-19, and UP-007 cells along 9 days of culture. Percentage of CFSE-labeled cells is given compared to an unstained control. B, Viability of U-87 MG, SNB-19, and UP-007 cells stained with CellTrace CFSE (5 μM) compared to a control of unstained cells. C, Percentage of Far Red^+ CHME3 cells along 9 days of culture. D, Viability of CHME3 stained with CellTrace (1 μM) when compared to a control of unstained cells. E, Histogram of the frequency of distributions of the labeling of $CFSE^+$ GBM cells showing a decrease of fluorescence intensity along the days of culture even though the whole cell population remains positive for CFSE. Mean ± SEM (N = 3, mean of three independent experiments). $P > .05$ when comparing cell viability of GBM or CHME-3 labeled cells (CFSE and Far Red, respectively) to unlabeled cells

percentage of CFSE$^+$ cells remained >95% for 7 days of culture showing no significant effects on cell viability. With GBM labeled with CFSE CellTrace, the human microglia cell line (CHME3) was labeled with a Far Red CellTrace to obtain a reliable labeling that allows a clear distinction between the two cell populations (GBM and MG). Using Far Red CellTrace (1 μM), MG cells remain Far Red$^+$ for 9 days in culture (Figure 1C) and viable when compared to unstained cells (Figure 1D). Fluorescence intensity of CellTrace dyes showed a decrease along the days of culture, as represented in Figure 1E, indicating that the cells remain proliferating passing the dye to the daughter cells. Figure 2 illustrates dot plots of a mixture of CFSE$^+$ GBM and Far Red$^+$ MG showing a complete and effective resolution of the two populations, which allows for a specific analysis of each of the populations in terms of viability, proliferation, and drug response.

3.2 | CHME3 cells display ability to be activated

To investigate the ability of CHME3 cells to respond an external stimulus, CHME3 cells were stimulated either with LPS and IFN-γ to drive a pro-inflammatory phenotype, or with IL-4 and IL-13 to drive an anti-inflammatory phenotype (Figure 3). Cell activation at the transcriptional level was studied by RT-qPCR, as shown in Figure 3A. When stimulated with LPS and IFN-ɣ for 48 hours, CHME3 cells showed an increased trend (relative to unstimulated cells—dashed line) for a raised expression for all cytokine genes examined. As expected, significant increases in expression were found for the pro-inflammatory cytokines: interleukin-1β (IL-1β, ~2.2-fold), interleukin-6 (IL-6, ~5.7-fold), interleukin-12 (IL-12, ~1.5-fold), C-X-C motif chemokine 10 (CXCL10, ~473-fold), and tumor necrosis factor alpha (TNF-α, ~2.1-fold) (Figure 3A). These results were further corroborated by cytokine array, which show an increased trend for the protein levels in stimulated CHME3 cells (Figure 3B). Pro-inflammatory cytokines CXCL10, IL-6, and TNF-α increased ~61.4-, 2.8-, and 1.6-fold, respectively, when stimulated with LPS and IFN-γ, as depicted in Figure 3B. Any alteration to IL-1β, IL-12, and IL-10 was observed with stimulation with LPS and IFN-γ. Compared to the unstimulated cells, activation of some anti-inflammatory cytokines was also evident, notably, C-C motif chemokine 22 (CCL22, ~2.0-fold), and the scavenger receptor, CD163 (~3.1-fold) (Figure 3A). When CHME3 cells were challenged with IL-4 and IL-13, there was also a trend for a raised expression for all cytokine genes examined, although that was less pronounced compared to the one seen with LPS and IFN-ɣ (Figure 3A). In terms of cytokine levels, when MG cells were stimulated with IL-4 and IL-13, a slight decrease of IL-1β, IL-6, IL-12, and IL-10 was observed; however, no alterations were found on CXCL10 and TNF-α (Figure 3B). The western blot data (Figure 3C,D) confirmed that CHME3 cells can display differential responsiveness following exposure to classical microglial activators. Here, the transcription factors characterizing microglial pro-inflammatory (STAT1, NF-kB p65) or anti-inflammatory (STAT6, STAT3) phenotypes were studied including their respective phosphorylation state. CHME3 cells, when exposed to LPS and INF-ɣ, showed an appropriate activation of pSTAT1 (~5.7-fold increase) and pNF-kB p65 (~2.5-fold increase). An exposure to IL-4 and IL-13 triggered appropriate activation of STAT6 (~49-fold increase) in CHME3 cells as observed by western blot. No alterations were observed in the levels of STAT3.

3.3 | MG support GBM growth and migration

To directly assess the effect of MG on GBM behavior, we established co-cultures of CFSE$^+$ GBM cells and Far Red$^+$

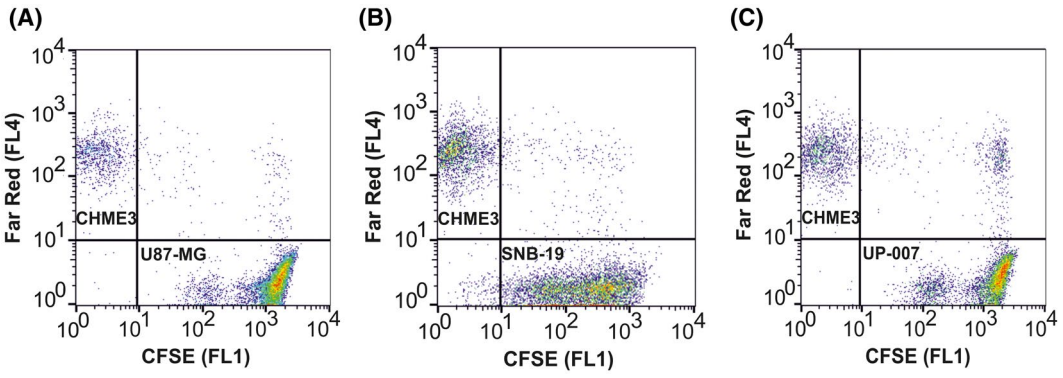

FIGURE 2 Two-dimensional dot plots showing mixed populations of CFSE$^+$ GBM and Far Red$^+$ MG. Dot plots illustrating mixtures of live Far Red$^+$ CHME3 cells with CFSE$^+$ U-87 MG (A), SNB-19 (B), and UP-007 (C) after 3 days of culture. The *X*-axis shows the intensity in the CFSE (FL1) channel and the *Y*-axis fluorescence intensity in the Far Red channel (FL4). The quadrants are defined by the intensity value of the unstained cells, which are within the lower left quadrant of the plots. Right bottom quadrant (CFSE$^+$/Far Red$^-$) comprises GBM cells, while left top quadrant (CFSE$^-$/Far Red$^+$) represents MG cells

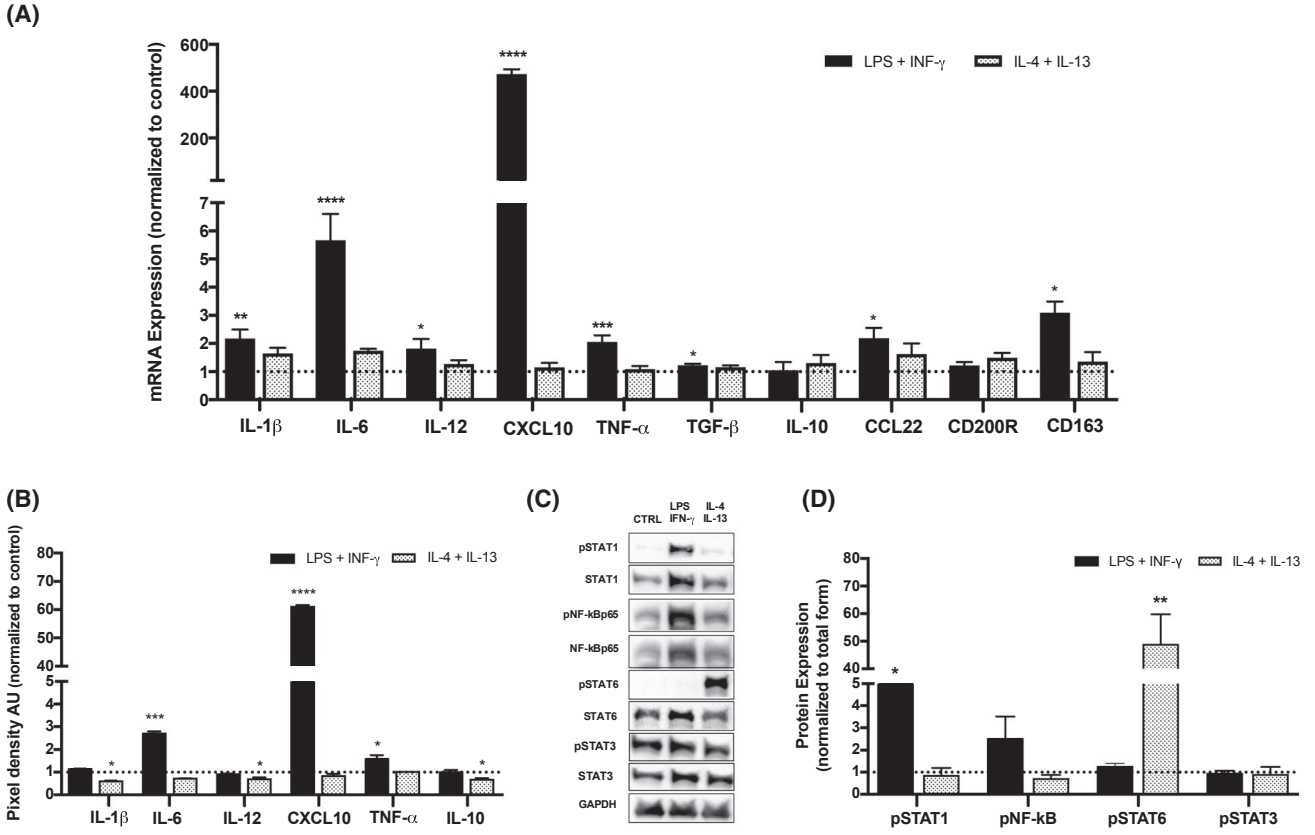

FIGURE 3 Polarization of CHME3 MG. A and B, mRNA expression (A) and soluble factors (B) from CHME3 cells either stimulated either with LPS and IFN-γ or IL-4 and IL-13. C and D, Phosphorylation of STAT1, NF-kB, STAT6, and STAT3 by CHME3 cells (C) and respective quantification (D). CHME3 cells were stimulated for 48 h either with LPS and IFN-ɣ toward pro-inflammatory or with IL-4 and IL-13 to induce an anti-inflammatory phenotype. Unstimulated cells were used as a control. Results normalized to unstimulated CHME3 cells. Mean ± SEM (N = 3, mean of three independent experiments). *$P < .05$, **$P < .01$, ***$P < .001$, ****$P < .0001$ compared to untreated CHME3 cells. The dashed lines in 3A, 3B, and 3D shows the respective level of normalized expression, that is, 1, in unstimulated CHME3 cells

MG at ratios of 90:10, 80:20, and 50:50. The rationale for the use of different GBM to MG ratios is based on the evidence that MG cells can be as high as 50% in a malignant brain tumor,[8] and that this percentage of MG rises with the grade of malignancy.[38] As a control, GBM and MG were grown in a monoculture. In all the tested co-culture ratios of GBM to MG cells, both cells presented the ability to grow together establishing close contact and, as displayed on Figure 4A, GBM and MG remained viable (viability >95%) in co-culture (Figure 4B). Furthermore, to study the effects of co-culture in both MG on GBM growth, fluorescence intensity of each CellTrace (CFSE or Far Red) was used as an indirect measure of cell proliferation following flow cytometry analysis (Figure 4C). In all three tested GBM cell lines, the presence of MG in culture resulted in an increase in cell proliferation of GBM (U-87 MG: ~17%; SNB-19: ~30%; UP-007: ~19% increase compared to monoculture of GBM, $P < .001$) at a higher percentage of MG cells (50% MG). Interestingly, SNB-19 cells demonstrated high proliferation ($P < .05$) even when cultured with a low percentage of MG (10%-20% MG).

Additionally, the effect of MG on GBM migration was assessed using scratch-wound and Transwell assays (Figure 5). Initially, we performed a scratch-wound assay on the three different GBM confluent cells either alone or in a contact co-culture with MG (Figure 4A, Supplemental Figure 1). As depicted on Figure 5A, U-87 MG and UP-007 when in a co-culture with MG showed no significant difference ($P > .05$) in terms of rate of closure of the gap compared to a monoculture of GBM. However, when comparing the co-cultures to a monoculture of MG, MG cells presented a statistically significant lower rate of closure. The lower rate of closure of MG might result in no differences between GBM in mono- and co-culture, which gives no clear results regarding migration of GBM cells. Nonetheless, the SNB-19 cells demonstrated a similar rate of closure to MG monoculture, which allows us to observe a significant effect on cell migration of SNB-19 when in co-culture with MG at a high percentage of MG (50%). In the presence of MG, SNB-19 migration in the wound-scratch assay showed a 1.73-fold increase in comparison to monocultures the SNB-19 (Figure 5A). To further

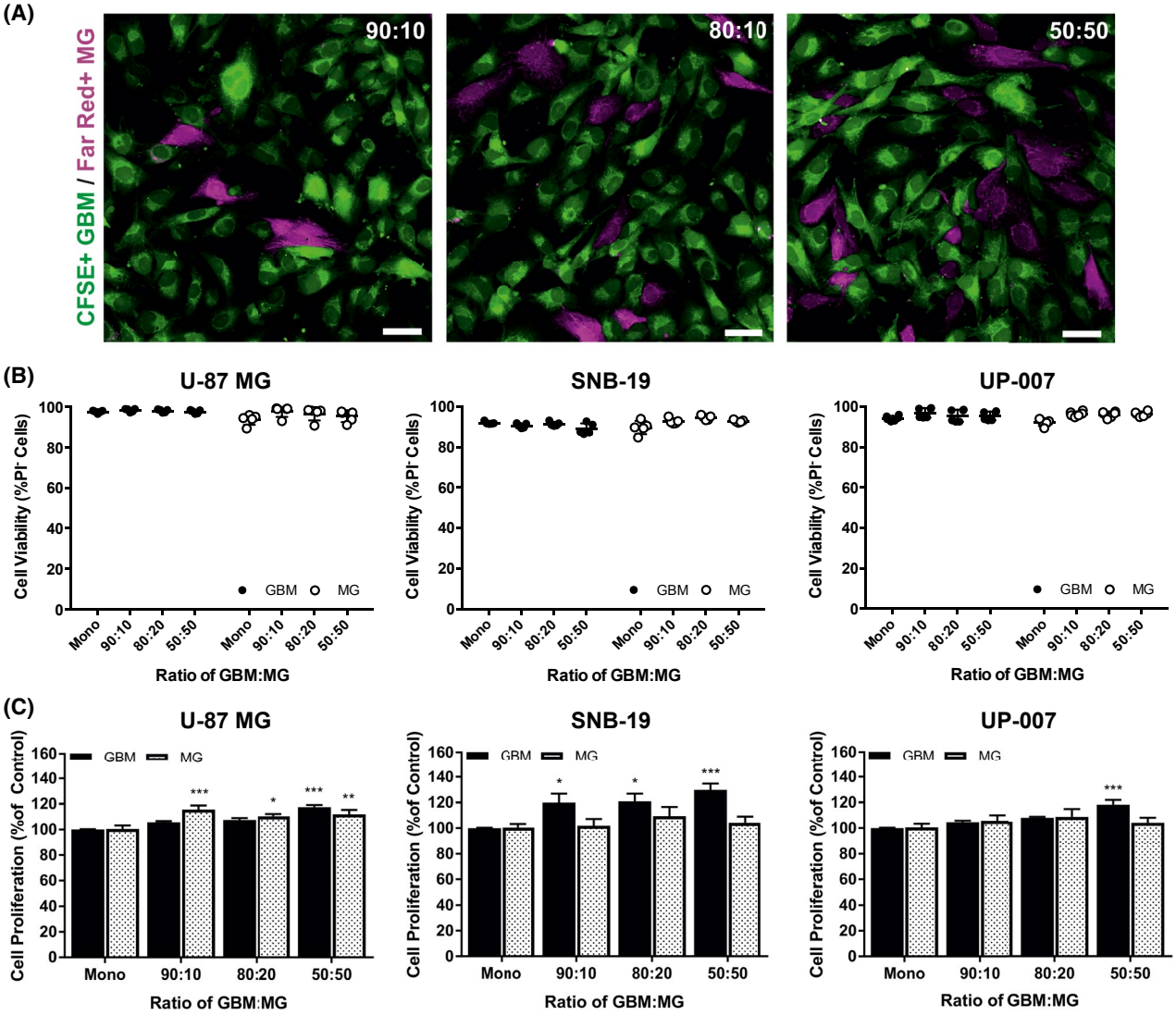

FIGURE 4 Viability and proliferation of GBM and MG cells growing in contact co-culture in 2D for 3 days. A, Representative images of $CFSE^+$ UP-007 and Far Red^+ CHME3 cells in co-culture at ratios of 90:10, 80:20, and 50:50 after 3 days of culture. Scale bar: 50 μm. B, Cell viability of U-87 MG, SNB-19, and UP-007 cells expressed as the percentage of propidium iodide (PI) negative cells quantified by flow cytometry. GBM cells culture in a contact co-culture with MG at a GBM:MG ratio of 90:10, 80:20, and 50:50. **C,** Proliferation of GBM and MG cells in contact co-culture at GBM:MG ratio of 90:10, 80:20, and 50:50 determined by flow cytometry. U-87 MG, SNB-19, and UP-007 proliferation expressed in relation to the control cells growing in a monoculture in 2D. Mean ± SEM (N = 3, mean of the three independent experiments). $^*P < .05$, $^{**}P < .01$, $^{***}P < .001$ compared to the monoculture either GBM or MG

clarify the role of MG on GBM migration, a Transwell assay was carried out (Figure 5B,C). We established the co-culture in the Transwell, in which GBM are seeded on top of the membrane and allowed to migrate toward the MG cells on the bottom compartment. Based on the results obtained in terms of GBM cell proliferation and migration at the different ratios of MG, co-cultures were tested at a ratio of 50:50 of GBM to MG for the three GBM cell lines. Migration of all GBM cells was significantly increased: U-87 MG, 1.45-fold ($P > .01$), SNB-19, 3.71-fold ($P > .001$), while UP-007, a 2.48-fold increase ($P > .001$), comparing to a culture of GBM without MG.

3.4 | MG modulates sensitivity to cytotoxics in GBM

Following the study on the influence of MG cells on the proliferation and migration of GBM, we tested the role of MG on the sensitivity to three cytotoxics (TMZ, CLM, and VCR) in the GBM cells (Figure 6). To obtain an effective dose for each drug, dose-response was carried out at a range of concentrations, and the IC_{50} values were obtained (Table 2, Supplemental Figure 2). In all GBM cell lines, treatment with TMZ (200-1000 μM) resulted in a reduction of cell viability up to ~75%-80% (Supplemental Figure 2), and with the range

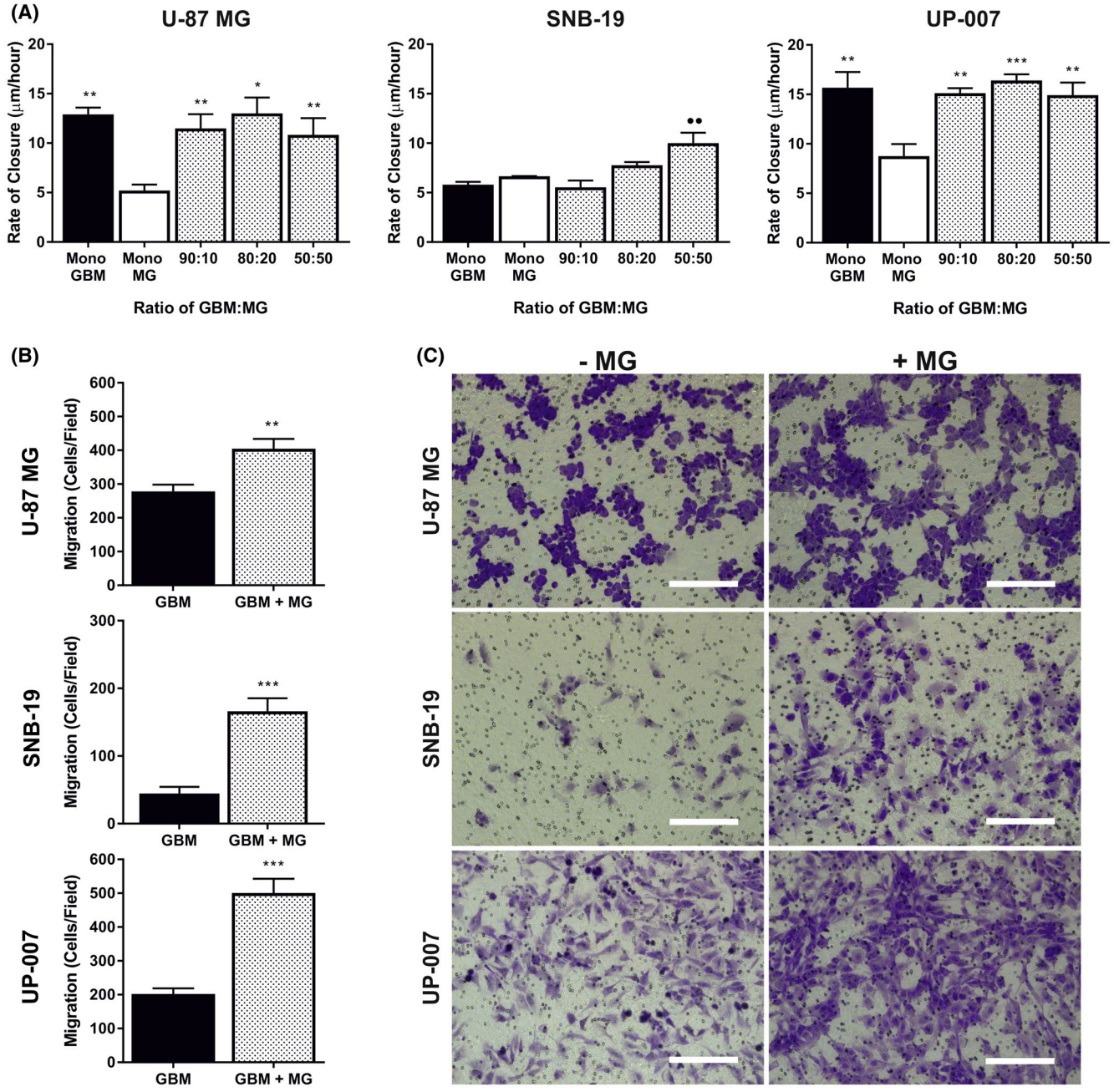

FIGURE 5 Migration of GBM in 2D co-cultures with MG cells. A, Rate of closure of the wound in a scratch assay with U-87 MG, SNB-19, and UP-007 co-cultures with MG at a GBM to MG ratio of 90:10, 80:20, and 50:50. The wound closure was followed for 18 h. B, Number of GBM migrating cells in a Transwell assay with U-87 MG, SNB-19, and UP-007 in co-culture with CHME3 at the ratio of 50:50. C, Representative micrographs of the migrating cells in Transwell assay containing U-87 MG, SNB-19, or UP-007 in co-culture with MG. Scale bar: 200 μm. Mean ± SEM (N = 3, mean of the three independent experiments). $^{\bullet\bullet}P < .01$ compared to the monoculture of SNB-19. $^{*}P < .05$, $^{**}P < .01$, $^{***}P < .001$ compared to monoculture of MG

of concentrations tested an IC_{50} value was not obtained. However, in CLM and VCR, the IC_{50} values for each cell line were calculated with CLM and VCR having IC_{50} values <30 μM (Table 2). Based on these results, a concentration within the IC_{50} range of CLM (20 μM) and VCR (2 μM) was used in GBM and MG co-cultures. For TMZ, the concentration of 400 μM was chosen for further studies. When treated with TMZ, the MG cells seemed not to statistically impact on sensitivity of GBM cells; however, a slight increase in proliferation of the GBM in co-culture with MG is observed (Figure 6A). On the other side, CLM- and VCR-treated GBM cells in co-culture with MG displayed a higher resistance to these cytotoxics even in the presence of a low amount of MG (10%-20%) (Figure 6B,C, $P < .05$).

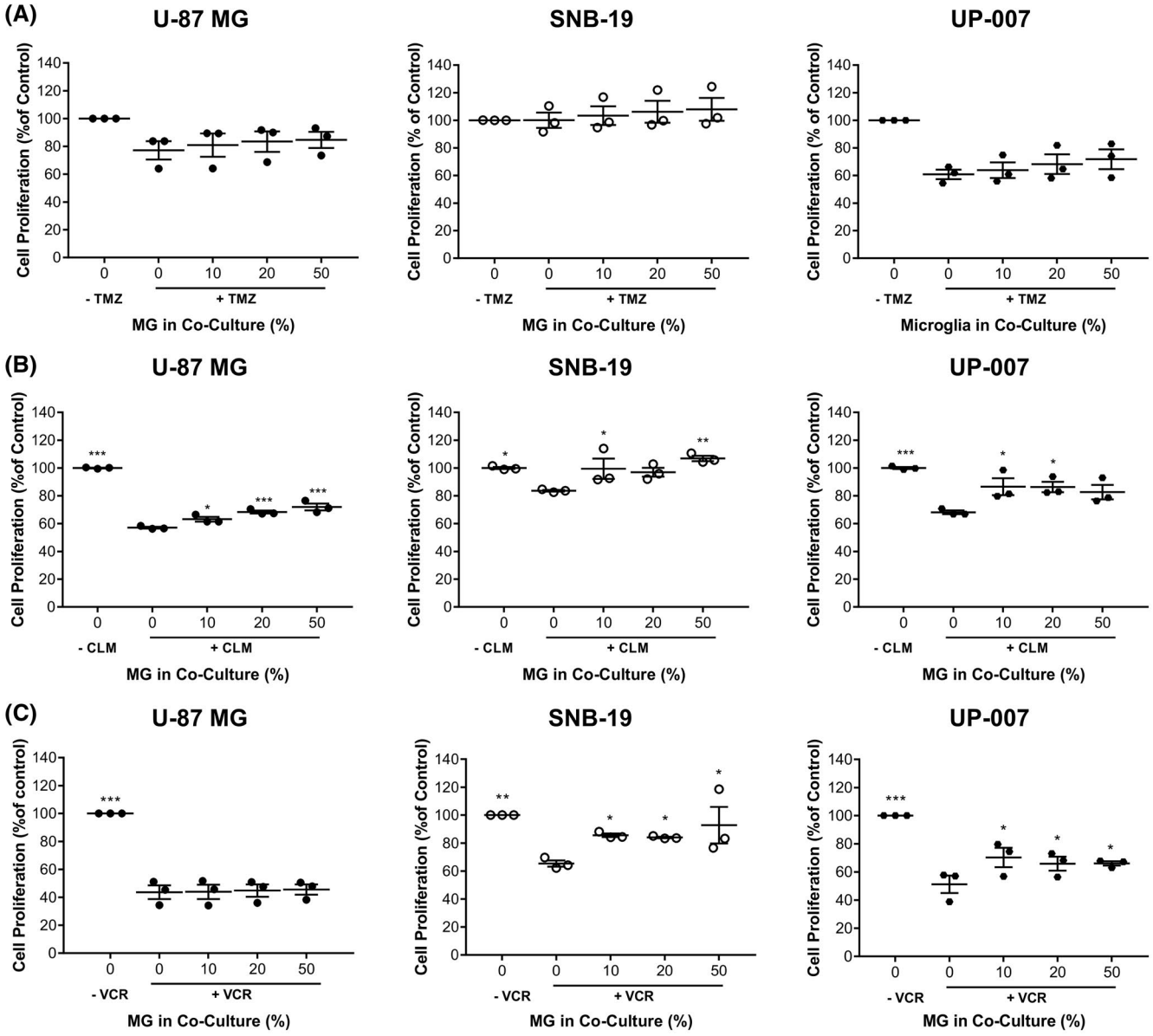

FIGURE 6 Response of GBM to TMZ, CLM, and VCR when in co-culture with ratios of MG in 2D. A, Proliferation of U-87 MG, SNB-19, and UP-00 in mono- or co-culture with MG when treated with TMZ at 400 μM for 2 days. B, U-87 MG, SNB-19, and UP-007 cell proliferation in a mono- or co-culture with MG after treated with CLM (20 μM) for 2 days. C, Proliferation of U-87 MG, SNB-19, and UP-007 cells in co-culture with MG when treated with VCR at 2 μM for 2 days. Co-cultures of GBM and MG were established at the ratios of 90:10, 80:20, and 50:50 of GBM to MG. Proliferation is expressed in relation to a control of GBM cells growing in monoculture. Mean ± SEM (N = 3, mean of the three independent experiments). *$P < .05$, **$P < .01$, ***$P < .001$ in comparison to monoculture of GBM

TABLE 2 IC_{50} values of TMZ, CLM, and VCR in three GBM cell lines and MG

	TMZ (μM)	CLM (μM)	VCR (μM)
GBM			
U-87 MG	>1000	16.37 ± 1.53	3.60 ± 0.62
SNB-19	>1000	27.83 ± 1.82	26.84 ± 17.45
UP-007	>1000	6.92 ± 1.77	6.48 ± 2.20
MG			
CHME3	>1000	4.42 ± 2.73	2.62 ± 0.56

3.5 | 3D co-culture model reflects influence of MG on GBM

The results obtained with the 2D co-cultures of GBM and MG demonstrated the effect of MG on the behavior of three GBM cell lines in human serum-supplemented media. Although these results demonstrate the relevance of non-neoplastic cells in in vitro models of GBM, the 3D environment is a key parameter to be considered. Thus, we established a 3D co-culture of GBM and MG by using a hyaluronic acid-based hydrogel aiming to mimic extracellular matrix (ECM)

of the tumor (Figure 7). As UP-007 cell line is a more realistic representation of a GBM, this biopsy-derived cell line was selected for the 3D studies using a ratio of GBM to MG of 50:50. In terms of cell viability, a Cell Triter 96 Cell Proliferation assay displays that cells, either in the mono- or co-culture, growing in 3D remained viable when comparing to the 2D cultures (Figure 7A). In addition, cells growing in the 3D system were stained for propidium iodide for calculation of dead cells (Figure 7B). The viability of GBM cells in the 3D hydrogel was not altered by the presence of MG (Figure 7B). However, in terms of cell proliferation, GBM cells growing in a co-culture with MG in 3D demonstrated greater proliferation (Figure 7C). Thus, these results reflect the data obtained in the 2D co-cultures, confirming that MG and GBM grown in close contact (Figure 7D) and that promotes proliferation of GBM. In 2D cultures, a ~19% increase in proliferation in GBM UP-007 cells was observed, while in the 3D culture in hyaluronic acid, a ~69% increase is obtained in a GBM to MG ratio of 50:50, suggesting that the 3D hyaluronic acid-based ECM further supports the role of MG in GBM.

The 3D co-culture model developed was challenged with TMZ, CLM, and VCR in order to establish a comparison to the 2D co-culture model (Figure 8). Cell viability was assessed by Cell Triter 96 Cell Proliferation assay of the mono- and co-cultures of GBM and MG at a ratio of 50:50 in 2D and 3D when treated with a dose of TMZ, CLM, or VCR. In the 3D environment, a dose of CLM and VCR

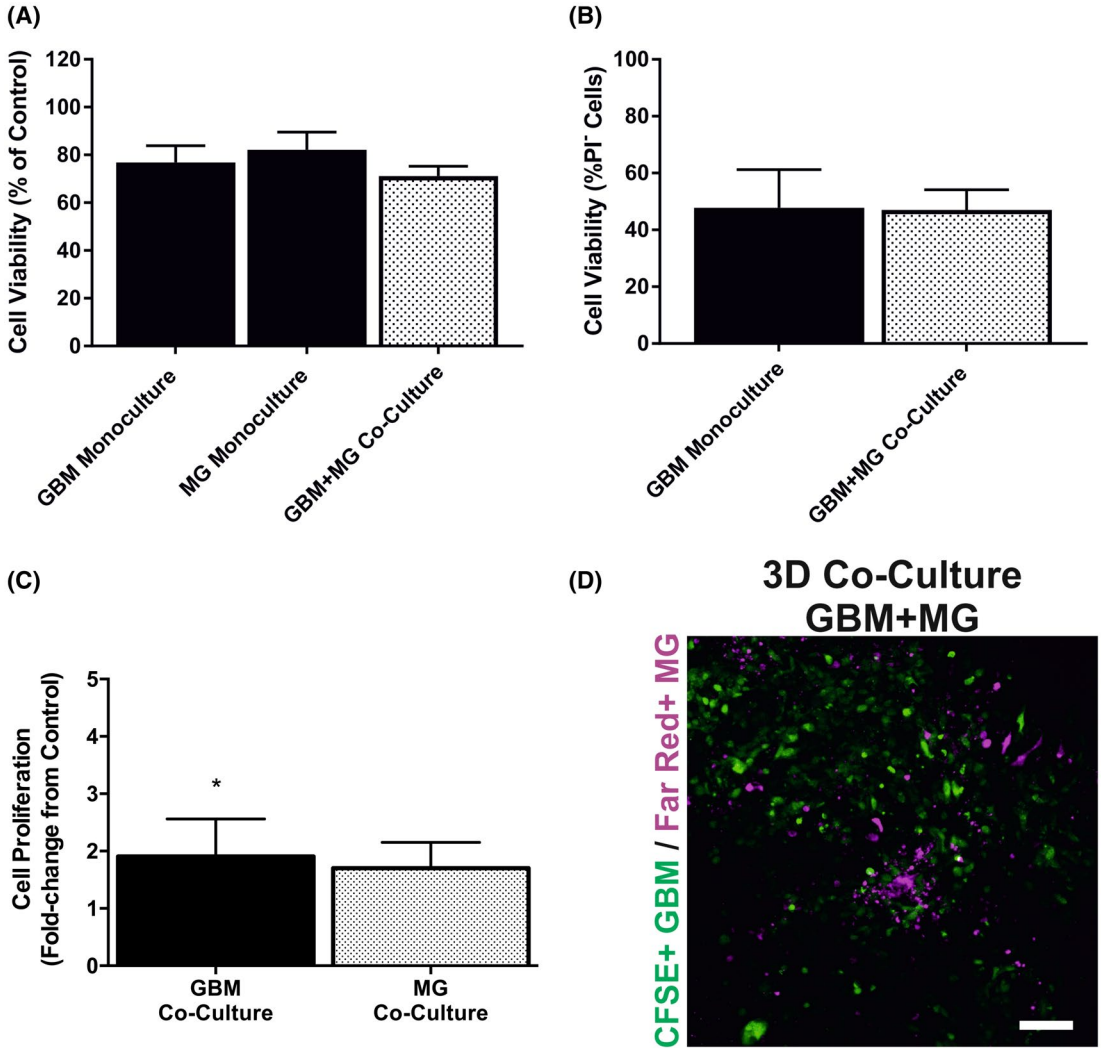

FIGURE 7 Cell viability and proliferation of GBM and MG cells in a 3D co-culture. A, Viability of mono- and co-cultures of GBM and MG in the hyaluronic acid hydrogel, HyStem-HP, compared to the 2D cultures. Viability was obtained by Cell Triter 96 Cell Proliferation assay after 3 days of culture. B, Viability of GBM cells in mono- or co-culture with MG in 3D system obtained by the number of propidium iodide (PI) negative GBM cells. C, Proliferation of GBM and MG cells in mono- or co-culture represented by the $CFSE^+$ GBM and Far Red^+ MG fluorescence. Fluorescence intensity is inversely related to proliferation. D, Representative image of a co-culture of UP-007 and CHME in 3D hydrogel. Scale bar: 100 μm. Mean ± SEM (N = 3). *$P < .05$ in comparison to monoculture of GBM

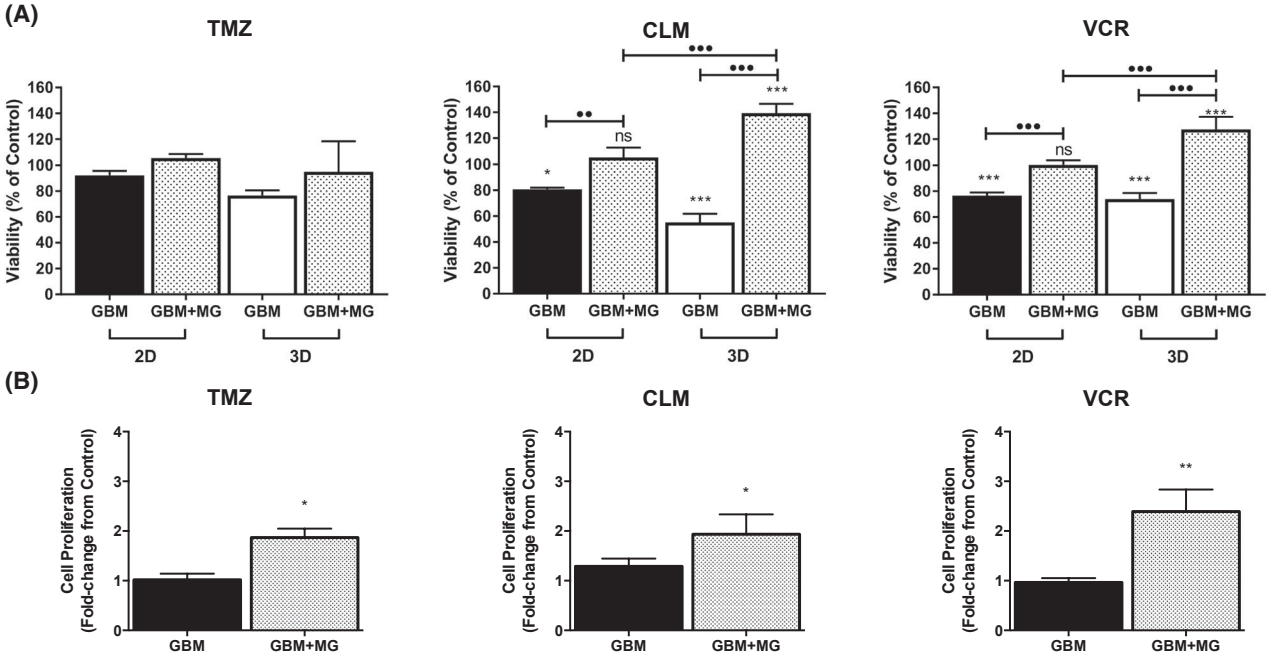

FIGURE 8 Drug response of GBM cells to TMZ, CLM, and VCR in 2D and 3D culture in mono- or co-culture with MG. A, Viability of UP-007 cells when treated with TMZ, CLM, or VCR obtained by Cell Triter 96 Cell Proliferation assay. Cells were either cultured in 2D or 3D conditions (HyStem-HP), alone or in co-culture with MG, at a 50:50 ratio for 1 day and treated with cytotoxics for 2 days. Cell viability was normalized with untreated cells for each of the model used (2D/3D and mono/co-culture). Mean ± SD (N = 3). $^{*}P < .05$, $^{***}P < .05$ in comparison to control (untreated cells). $^{\bullet\bullet}P < .01$, $^{\bullet\bullet\bullet}P < .001$, as indicated in the figure. B, Corrected total cell fluorescence of GBM cultured in 3D treated with TMZ, CLM, or VCR either in mono- or co-culture with MG. Fluorescence intensity is inversely related to proliferation. Mean ± SEM (N = 6). $^{*}P < .05$, $^{**}P < .01$ comparison to monoculture treated with the TMZ, CLM, or VCR

triggered the decrease of cell viability of GBM; however, a co-culture with MG caused the survival of >100% of the population in response to the CLM and VCR (Figure 8A). GBM and MG co-cultured in the hydrogel exhibit a 2.5- and 1.7-fold increase in cell viability comparing to the monoculture of GBM in 3D when treated with CLM and VCR, respectively ($P < .001$). The addition of TMZ resulted in no statistically significant difference in the mono- and co-cultures (Figure 8A, $P > .05$); however, a slight increase in viability is observed when comparing both conditions in 2D and 3D. Although these results in terms of cell viability appear to illustrate the drug resistance of GBM when in contact with MG, the Cell Triter 96 Cell Proliferation assay gives an overall viability of the whole co-culture system and not a specific effect on the GBM. In order to further elucidate the response of GBM, cell fluorescence intensity of $CFSE^{+}$ UP-007 cells treated with TMZ, CLM, and VCR was quantified as a measure of cell proliferation (Figure 8B). In terms of cell proliferation, the dose of TMZ, CLM, or VCR did not have a statistically significant effect on the monoculture of UP-007 in 3D ($P > .05$). Nevertheless, when comparing the treated mono- and co-cultures in 3D, a significant reduction of cell fluorescence was noted for all drugs, thus confirming a role for MG in GBM resistance.

4 | DISCUSSION

Currently, little is known about the role of non-neoplastic cells, such as MG cells, and ECM in GBM behavior and response to cytotoxics. To understand the impact of MG cells in GBM, we established a co-culture model comprising both human GBM (U-87 MG, SNB-19, or UP-007) and MG (CHME3) cells cultured under human serum supplementation. CHME3 is a human MG cell line able to respond to environmental stimuli. Here, we showed the CHME3 cells to be responsive to classical pro-inflammatory signal through the Toll-like 4 receptor (TLR4) stimulation by LPS and IFN-γ, leading to activation of STAT1 and the nuclear factor-kB (NF-kB). This pathway is typically associated with microglial release of IL-1β, IL-12, TNF-α, and IL-6, and with high receptor expression for CD80, CD86, and CXCL10. In contrast, IL-4 receptor and IL-10 receptor stimulation leads to activation of STAT6 and STAT3 signaling, respectively, and is typically associated with microglial release of IL-10, TGF-β, IL-4, the C-C motif chemokine ligand 22 (CCL22) and transglutaminase 2 (TGM2), followed by expression of several receptors, including class A scavenger (SR-A, CD204) and mannose receptor (CD206), CD163, and CD200R.[38]

Initially, the co-cultures of GBM and MG were explored in 2D using a range of ratios of GBM to MG (90:10, 80:20, 50:50), and then the model was translated to 3D using a hyaluronic acid hydrogel to mimic the GBM microenvironment and comprehend the role of ECM in combination with non-neoplastic MG cells. Using three GBM cell lines, including an in house established biopsy, we aimed to evaluate the influence of tumor heterogeneity in the response to MG. With co-cultures under human serum supplementation, the initial study focused on the identification of the different cell types when co-culturing GBM and MG. To do so, GBM and MG cells were stained using two amine-reactive dyes, CellTrace CFSE and Far Red. These amine-reactive dyes have been described to be superior in peak resolution and for a non-specific dye transfer compared to the membrane-staining dyes.[39,40] CellTrace CFSE and Far Red dyes permeate live cells and fluorescently label proteins through covalent interactions with amine groups.[41] Additionally, CellTrace dyes allow tracking the cell proliferation, as at each cell division, fluorescence intensity is halved in the daughter cells.[40] Thus, CellTrace CFSE and Far Red are not only useful to label cells but also to track and measure cell proliferation. Our results confirmed that CFSE (5 μM) is able to label the GBM cells (~99% of $CFSE^+$ GBM up to 7 days in culture) without causing an effect in cell viability. Similarly, CellTrace Far Red (1 μM) was sufficient to stain MG cells maintaining them viable when compared to unstained controls. Analysis by flow cytometry demonstrated that both cell types are specifically labeled, and identification of each cell type is possible in a mixture of GBM and MG.

In the past couple of decades, glioma infiltrating MG have been described to secrete factors, as cytokines, growth factors and proteases, which directly or indirectly influence a glioma growth.[8,42] In GBM, MG cells have been shown to promote cell proliferation, and also migration in in vitro non-contact co-cultures or by using MG conditioned media.[12,13,15,43] The exact mechanism is still unclear, however microglial stress inducible protein 1 was to shown to be implicated in GBM progression in the presence of MG.[13] Although MG cells promote tumor progression, their influence in the human GBM drug-response has not yet been described. We therefore investigated the influence of MG cells in GBM proliferation and migration in 2D contact co-cultures with three different GBM cell lines. Additionally, to comprehend the significance of MG cells in drug-response of GBM cells, co-cultures were challenged with cytotoxics (TMZ, CLM, and VCR). TMZ is the standard treatment of GBM acting by addition of methyl groups to purine bases of DNA,[2] and VCR is a vinca alkaloid that interacts with β-tubulin inhibiting mitosis.[44] CLM is tricyclic antidepressant that has been shown to have selective cytotoxicity against glioma cells in vitro by acting via mitochondria and mediating apoptosis[45-47] and autophagy.[28,29] CLM was included since not only has been reported to act on the GBM cells through a completely different, mitochondrial, mechanism[28,48-50] but because a sophisticated 3D human in vitro drug testing model may provide a non-live animal means to "fast-track" re-purposed drugs to clinic for GBM treatment. Indeed, CLM has already been demonstrated, some evidence of good tolerance and efficacy in small/anecdotal patient cohorts with 80.8% of patients from a cohort of 27 showing good partial response both clinically and radiologically.[51]

In our studies, GBM and MG co-cultures were established at a ratio from 10% to 50% of MG in culture to mimic the in vivo levels of MG and, possibly, to correlate the level of MG with the malignancy of GBM. All ratios of GBM to MG demonstrated that both cell types grow in close contact and remain viable (>95% viability) for the tested days of co-culture. Interestingly, the GBM cells growing in close contact with MG revealed a modest increase in proliferation (15%-30% increase within the three GBM cells). Our data confirms the previous reports showing the influence of MG in GBM.[13,15] Fonseca and co-workers, using conditioned media from primary mouse MG and in house human GBM cell line reported influence of MG in tumor proliferation (~2-fold increase in MG conditioned media condition).[13] Additionally, Zhai et al [15] also described that the growth rate of mouse GL261 GBM is modestly higher when co-cultured with primary mouse MG (15.3% increase). Although both studies highlight the influence of MG, it is relevant to consider that these studies describe mouse cells, while our studies are focused on human cells cultured in human-derived serum. Based on these data, we further considered the influence of MG in the migration of GBM. Three GBM cells revealed a greater migration when in culture with MG, as previously reported in mouse cell cultures.[12] When challenged with cytotoxic agents, GBM cells showed an increase in proliferation when in contact with MG. Our studies show that even a low amount of MG (10%-20%) is able to confer resistance of GBM to cytotoxics. Little is known regarding the role of non-neoplastic cells, particularly, MG in resistance of GBM. Previous studies.[52,53] have described that astrocytes induce drug resistance. Using a panel of human GBM cells constitutively expressing a fusion transgene encoding luciferase and the enhanced green fluorescence protein (eGFP), co-cultures of eGFP/Luciferase GBM, and astrocytes were explored as a model for drug screening.[53] Experiments demonstrated that the presence of astrocytes mediated a significantly higher cell survival after TMZ treatment in U251, C6, and A172 GBM cell lines and also doxorubicin treatment in certain cell lines (U251 and LN-18). In a subsequent study, a co-culture was established using human astrocytes and GBM cells to comprehend the protective mechanisms of astrocytes.[52] In response to TMZ and VCR, astrocytes were able to reduce glioma cell apoptosis induced by these drugs owing to the

direct contact between astrocytes and glioma, mainly, mediated through connexion 43 gap junctions.[52] Recently, using a 3D matrix comprised of oligomer type-I collagen and hyaluronan, Herrera-Perez and co-workers established cultures of patient-derived GBM cells with human astrocytes and endothelial precursors in 3D.[54] Migration analysis of GBM cells within the 3D in vitro model demonstrated that the presence of astrocytes significantly increases the migration of GBM, while presence of endothelial precursors has varied effects on the migration of different GBM cell lines. Although the influence of astrocytes in GBM drug resistance is becoming clear, we unrevealed the unknown role of MG in a range of human GBM cell lines suggesting the relevance of the incorporation of MG cells in novel in vitro models for drug screening.

Based on our results showing the protective effect of MG on GBM, we established the 3D in vitro model comprising the co-culture of GBM and MG in a hyaluronic acid-based hydrogel for drug screening. As observed in the 2D experiments, MG cells influenced GBM growth and, specially, in the 3D ECM a greater proliferation rate was obtained in the co-culture in comparison to monoculture of GBM. Using this in vitro 3D model, drug resistance to CLM and VCR was shown to be attenuated by the presence of MG cells in a greater extent than the resistance observed in 2D culture conditions. Bioengineered hydrogels with brain-mimicking biochemical and mechanical properties have been described for 3D in vitro models of GBM.[36,55,56] In particular, hyaluronic acid-based hydrogels have been shown to support GBM cells (U-87 MG) maintaining them viable, active, and responsive to matrix-immobilized hyaluronic acid leading to the upregulation of genes associated with matrix remodeling and tumor growth.[36,55,57] Few studies, however, have explored the culture of GBM with non-neoplastic cells in a 3D condition for assessment of drug response. Using a 3D matrix of collagen-hyaluronan, patient-derived GBM cells in co-culture with astrocytes and endothelial cells treated with SH-4-54 (small molecule signal transducer and activator of transcription, STAT3, inhibitor) showed a ~100% survival, while 80% and 38% survival was obtained with 3D ECM with no stromal cells and 2D monolayers, respectively.[54]

Here, we investigated the influence of the in vitro tumor microenvironment comprised of 3D matrix and non-neoplastic cells (MG) on the growth, proliferation, and resistance to cytotoxic drugs of various human GBM cell lines. Our results confirm the role of MG in GBM behavior using human cell lines cultured in human serum-based conditions and validate the use of in vitro controllable platforms that recapitulate the microenvironment of GBM as powerful tools for cancer studies. This work represents the first in a series which are planned to report on the systematic development of 3D human models of brain/GBM microenvironment for preclinical testing of therapeutics, providing a non-laboratory animal approach to better reflect the unique conditions inherent within the human brain. Our studies in both 2D and 3D concerning the influence of MG on GBM drug sensitivity, which are reported herein will be further established to test the role of non-neoplastic astrocytes, as well as, pericytes and hyperplastic endothelial cells obtained from biopsies from GBM glomerular microvascular proliferation/endothelial hyperplasia regions. Moreover, since stem cell phenotypes are present in patient xenograft models,[58] GBM cell populations reflecting standard and stem cell phenotypes will be used in our ultimate human 3D preclinical drug-testing models. We are also planning on exploring human patient-derived, induced pluripotent stem cells (iPSCs), which have been reported to show great promise in engineering models,[59] and can provide a more realistic representation of human disease and treatment response than the established cell culture and animal models. Moreover, within these human iPSC-based 3D preclinical testing models, we can use gene silencing approaches of key genes that regulate the pathways of therapeutic sensitivity and resistance. Indeed, such approaches have already been utilized in in vitro organoids of a few different cancers for elucidation of regulators of tumorigenesis and therapeutic sensitivity.[60] The information within this paper therefore paves the way for a new era heralding improvement in the preclinical testing of therapeutics for malignant brain tumors using manipulated, 3D human in vitro models which better represent a clinical situation than existing laboratory animal models which have hitherto be designated as "gold standards."

ACKNOWLEDGMENTS

The study was kindly funded by the Jake McCarthy Foundation. The Brain Tumour Research Centre at the University of Portsmouth is also core funded by the charity, Brain Tumour Research and receives funding for its 3D human in vitro modeling program from Animal Free Research, UK. Collaborative research between the University of Cardiff and the University of Portsmouth was supported by Cancer Research Wales, the University of Cardiff and Brain Tumour Research. BZB was supported by an EU Erasmus studentship, PC was supported by the University of Pisa. The authors also thank Professor Brian Bigger from the University of Manchester for kindly providing the human microglial cells (CHME3).

CONFLICT OF INTEREST

The authors declare that they have no competing interests.

AUTHOR CONTRIBUTIONS

D.M. Leite, M. Gumbleton, and G.J. Pilkington designed research; D.M. Leite, B.Z. Baskovic, P. Civita, and C. Neto

performed the research; D.M. Leite and C. Neto analyzed data; and D.M. Leite and G.J. Pilkington wrote the paper.

REFERENCES

1. Ostrom QT, Bauchet L, Davis FG, et al. The epidemiology of glioma in adults: a "state of the science" review. *Neuro-Oncology*. 2014;16:896-913.
2. Stupp R, Mason WP, van den Bent MJ, et al. Radiotherapy plus concomitant and adjuvant temozolomide for glioblastoma. *N Engl J Med*. 2005;352:987-996.
3. Bellail AC, Hunter SB, Brat DJ, Tan C, Van Meir EG. Microregional extracellular matrix heterogeneity in brain modulates glioma cell invasion. *The international journal of biochemistry & cell biology*. 2004;36:1046-1069.
4. Zamecnik J. The extracellular space and matrix of gliomas. *Acta Neuropathol*. 2005;110:435-442.
5. Rape A, Ananthanarayanan B, Kumar S. Engineering strategies to mimic the glioblastoma microenvironment. *Adv Drug Deliv Rev*. 2014;79–80:172-183.
6. Xiao W, Sohrabi A, Seidlits SK. Integrating the glioblastoma microenvironment into engineered experimental models. *Future Science OA*. 2017;3:FSO189.
7. Charles NA, Holland EC, Gilbertson R, Glass R, Kettenmann H. The brain tumor microenvironment. *Glia*. 2011;59:1169-1180.
8. Hambardzumyan D, Gutmann DH, Kettenmann H. The role of microglia and macrophages in glioma maintenance and progression. *Nat Neurosci*. 2016;19:20-27.
9. Junttila IS, Mizukami K, Dickensheets H, et al. Tuning sensitivity to IL-4 and IL-13: differential expression of IL-4Ralpha, IL-13Ralpha1, and gammac regulates relative cytokine sensitivity. *J Exp Med*. 2008;205:2595-2608.
10. Lisi L, Stigliano E, Lauriola L, Navarra P, Dello Russo C. Proinflammatory-activated glioma cells induce a switch in microglial polarization and activation status, from a predominant M2b phenotype to a mixture of M1 and M2a/B polarized cells. *ASN Neuro*. 2014;6:e00144.
11. Orihuela R, McPherson CA, Harry GJ. Microglial M1/M2 polarization and metabolic states. *Br J Pharmacol*. 2016;173:649-665.
12. Bettinger I, Thanos S, Paulus W. Microglia promote glioma migration. *Acta Neuropathol*. 2002;103:351-355.
13. Fonseca AC, Romao L, Amaral RF, et al. Microglial stress inducible protein 1 promotes proliferation and migration in human glioblastoma cells. *Neuroscience*. 2012;200:130-141.
14. Rolón-Reyes K, Kucheryavykh YV, Cubano LA, et al. Microglia activate migration of glioma cells through a Pyk2 intracellular pathway. *PLoS ONE*. 2015;10:e0131059.
15. Zhai H, Heppner FL, Tsirka SE. Microglia/macrophages promote glioma progression. *Glia*. 2011;59:472-485.
16. Koh I, Cha J, Park J, Choi J, Kang S-G, Kim P. The mode and dynamics of glioblastoma cell invasion into a decellularized tissue-derived extracellular matrix-based three-dimensional tumor model. *Sci Rep*. 2018;8:4608.
17. Yoo K-C, Suh Y, An Y, et al. Proinvasive extracellular matrix remodeling in tumor microenvironment in response to radiation. *Oncogene*. 2018;37:3317-3328.
18. Gomez-Roman N, Stevenson K, Gilmour L, Hamilton G, Chalmers AJ. A novel 3D human glioblastoma cell culture system for modeling drug and radiation responses. *Neuro-Oncology*. 2017;19:229-241.
19. Day AJ, Prestwich GD. Hyaluronan-binding proteins: tying up the giant. *J Biol Chem*. 2002;277:4585-4588.
20. Jadin L, Pastorino S, Symons R, et al. Hyaluronan expression in primary and secondary brain tumors. *Ann Transl Med*. 2015;3:1-8.
21. Park JB, Kwak H-J, Lee S-H. Role of hyaluronan in glioma invasion. *Cell Adh Migr*. 2008;2:202-207.
22. Emerman JT, Fiedler EE, Tolcher AW, Rebbeck PM. Effects of defined medium, fetal bovine serum, and human serum on growth and chemosensitivities of human breast cancer cells in primary culture: inference for in vitro assays. *Vitro Cell Dev Biol*. 1987;23:134-140.
23. Murray SA. *Significance of serum supplementation type on gene and protein expression in human glioma cells in vitro*. Portsmouth: PhD, University of Portsmouth; 2010.
24. Bolteus AJ, Berens ME, Pilkington GJ. Migration and invasion in brain neoplasms. *Curr Neurol Neurosci Rep*. 2001;1:225-232.
25. Maherally Z, Fillmore HL, Tan SL, et al. Real-time acquisition of transendothelial electrical resistance in an all-human, in vitro, 3-dimensional, blood-brain barrier model exemplifies tight-junction integrity. *FASEB*. 2018;32:168-182.
26. Jassam SA, Maherally Z, Smith JR, et al. TNF-α enhancement of CD62E mediates adhesion of non-small cell lung cancer cells to brain endothelium via CD15 in lung-brain metastasis. *Neuro Oncology*. 2016;18:679-690.
27. Jassam SA, Maherally Z, Smith JR, et al. CD15s/CD62E interaction mediates the adhesion of non-small cell lung cancer cells on brain endothelial cells: implications for cerebral metastasis. *Int J Mol Sci*. 2017;18:E1474.
28. Shchors K, Massaras A, Hanahan D. Dual targeting of the autophagic regulatory circuitry in gliomas with repurposed drugs elicits cell-lethal autophagy and therapeutic benefit. *Cancer Cell*. 2015;28:456-471.
29. Howarth A, Madureira PA, Lockwood G, et al. Modulating autophagy as a therapeutic strategy for the treatment of paediatric high-grade glioma. *Brain Pathol*. 2019;1-19.
30. Hill R, Murray SA, Maherally Z, Higgins SC, Pilkington GJ. Drug repurposing to circumvent chemotherapy resistance in brain tumours. In: Tivan A, ed. *Resistance to targeted therapies against adult brain cancers*. Cham, Switzerland: Springer International Publishing; 2016:107-144.
31. Plowman J, Waud WR, Koutsoukos AD, Rubinstein LV, Moore TD, Grever MR. Grever preclinical antitumor activity of temozolomide in mice: efficacy against human brain tumor xenografts and synergism with 1,3-Bis(2-chloroethyl)-1-nitrosourea. *Can Res*. 1994;54:3793-3799.
32. Boyle FM, Eller SL, Grossman SA. Penetration of intra-arterially administered vincristine in experimental brain tumor. *Neuro Oncology*. 2004;6:300-306.
33. Janabi N, Peudenier S, Héron B, Ng KH, Tardieu M. Establishment of human microglial cell lines after transfection of primary cultures of embryonic microglial cells with the SV40 large T antigen. *Neurosci Lett*. 1995;195:105-108.
34. An Q, Fillmore HL, Vouri M, Pilkington GJ. Brain tumor cell line authentication, an efficient alternative to capillary electrophoresis by using a microfluidics-based system. *Neuro Oncology*. 2014;16:265-273.
35. Livak KJ, Schmittgen TD. Analysis of relative gene expression data using real-time quantitative PCR and the 2(Delta Delra C(T)) method. *Methods*. 2001;25:402-408.

36. Pedron S, Becka E, Harley BA. Regulation of glioma cell phenotype in 3D matrices by hyaluronic acid. *Biomaterials*. 2013;34:7408-7417.
37. Jensen EC. Quantitative analysis of histological staining and fluorescence using ImageJ. *The Anatomical Record*. 2013;296:378-381.
38. Komohara Y, Ohnishi K, Kuratsu J, Takeya M. Possible involvement of the M2 anti-inflammatory macrophage phenotype in growth of human gliomas. *J Pathol*. 2008;216:15-24.
39. Begum J, Day W, Henderson C, et al. A method for evaluating the use of fluorescent dyes to track proliferation in cell lines by dye dilution. *Cytometry A*. 2013;83:1085-1095.
40. Ivanov DP, Parker TL, Walker DA, et al. In vitro co-culture model of medulloblastoma and human neural stem cells for drug delivery assessment. *J Biotechnol*. 2015;205:3-13.
41. Lyons AB. Divided we stand: tracking cell proliferation with carboxyfluorescein diacetate succinimidyl ester. *Immunol Cell Biol*. 1999;77:509-515.
42. Graeber MB, Scheithauer BW, Kreutzberg GW. Microglia in brain tumors. *Glia*. 2002;40:252-259.
43. Zhu W, Carney KE, Pigott VM, et al. Glioma-mediated microglial activation promotes glioma proliferation and migration: roles of Na+/H+ exchanger isoform 1. *Carcinogenesis*. 2016;37:839-851.
44. Jordan MA, Wilson L. Microtubules as a target for anticancer drugs. *Nat Rev Cancer*. 2004;4:253-265.
45. Higgins SC, Alagbaoso A, Javid T, et al. P08.57 Involvement of both the extrinsic and intrinsic apoptotic pathways with clomipramine treatment of human glioblastoma cells under normoxic and hypoxic conditions. *Neuro-oncology*. 2016;18:iv54-iv55.
46. Parker KA, Pilkington GJ. Apoptosis of human malignant glioma-derived cell cultures treated with clomipramine hydrochloride as detected by annexin V assay. *Radiology and Oncology*. 2006;40:87-93.
47. Pilkington GJ, Akinwunmi J, Amar S. The role of tricyclic drugs in selective triggering of mitochondrially mediated apoptosis in neoplastic glia: a therapeutic option in malignant glioma? *Radiology and Oncology*. 2006;40:73-85.
48. Daley E, Wilkie D, Loesch A, et al. Chlorimipramine: a novel anticancer agent with a mitochondrial target. *Biochem Biophys Res Comm*. 2005;328:623-632.
49. Meredith EJ, Holder MJ, Chamba A, et al. The serotonin transporter (SLC6A4) is present in B-cell clones of diverse malignant origin: probing a potential anti-tumor target for psychotropics. *FASEB*. 2005;19:1187-1189.
50. Pilkington GJ, Parker K, Murray SA. Approaches to mitochondrially mediated cancer therapy. *Semin Cancer Biol*. 2008;18:226-235.
51. Beaney RP, Gullan RW, Pilkington GJ. Therapeutic potential of antidepressants on malignant glioma: clinical experience with clomipramine. *Journal of Clinical Oncoloyg*. 2005;23:1535.
52. Chen W, Wang D, Du X, et al. Glioma cells escaped from cytotoxicity of temozolomide and vincristine by communicating with human astrocytes. *Med Oncol*. 2015;32:1-13.
53. Yang N, Yan T, Zhu H, et al. A co-culture model with brain tumor-specific bioluminescence demonstrates astrocyte-induced drug resistance in glioblastoma. *J Transl Med*. 2014;12:1-9.
54. Herrera-Perez RM, Voytik-Harbin SL, Sarkaria JN, Pollok KE, Fishel ML, Rickus JL. Presence of stromal cells in a bioengineered tumor microenvironment alters glioblastoma migration and response to STAT3 inhibition. *PLoS ONE*. 2018;13:e0194183.
55. Pedron S, Hanselman JS, Schroeder MA, Sarkaria JN, Harley BAC. Extracellular hyaluronic acid influences the efficacy of EGFR tyrosine kinase inhibitors in a biomaterial model of glioblastoma. *Adv Healthcare Mater*. 2017;6:1-9.
56. Wang C, Tong X, Yang F. Bioengineered 3D brain tumor model to elucidate the effects of matrix stiffness on glioblastoma cell behavior using PEG-based hydrogels. *Mol Pharm*. 2014;11:2115-2125.
57. Rao SS, Dejesus J, Short AR, Otero JJ, Sarkar A, Winter JO. Glioblastoma behaviors in three-dimensional collagen-hyaluronan composite hydrogels. *ACS Appl Mater Interfaces*. 2013;5:9276-9284.
58. Leiss L, Mutlu E, Øyan A, et al. Tumour-associated glial host cells display a stem-like phenotype with a distinct gene expression profile and promote growth of GBM xenografts. *BMC Cancer*. 2017;17:1-13.
59. Papapetrou EP. Patient-derived induced pluripotent stem cells in cancer research and precision oncology. *Nat Med*. 2016;22:1392-1401.
60. Smith RC, Tabar V. Constructing and deconstructing cancers using human pluripotent stem cells and organoids. *Cell Stem Cell*. 2019;24:12-24.

SUPPORTING INFORMATION

Additional supporting information may be found online in the Supporting Information section.

How to cite this article: Leite DM, Zvar Baskovic B, Civita P, Neto C, Gumbleton M, Pilkington GJ. A human co-culture cell model incorporating microglia supports glioblastoma growth and migration, and confers resistance to cytotoxics. *The FASEB Journal*. 2019;00:1–18. https://doi.org/10.1096/fj.201901858RR